



Quantifying Autophagosomes and Autolysosomes in Cells Using Imaging Flow Cytometry

Robin Rajan,¹ Magdalena Karbowniczek,¹ Haley R. Pugsley,² Manoj K. Sabnani,¹ Aristotelis Astrinidis,¹ Ninh M. La-Beck^{1*}

¹School of Pharmacy, Department of Immunotherapeutics and Biotechnology, Texas Tech University Health Sciences Center, Abilene, Texas

²Amnis Corporation, EMD Millipore, Seattle, Washington

Received 17 September 2014; Revised 26 January 2015; Accepted 10 February 2015

Additional Supporting Information may be found in the online version of this article.

Grant sponsor: Cancer Prevention Research Institute of Texas (CPRIT), Grant number: 120168 (to MK)

Correspondence to: Ninh M. La-Beck, Pharm.D, Assistant Professor, Department of Immunotherapeutics and Biotechnology, Texas Tech University Health Sciences Center-School of Pharmacy, 1718 Pine Street, Abilene, TX 79601. E-mail: irene.la-beck@ttuhsc.edu

Conflict of interest and disclosures: HRP is an employee of Amnis Corporation. All other authors declare that they have no conflicts of interests and no financial disclosures.

Published online 27 February 2015 in Wiley Online Library (wileyonlinelibrary.com)

DOI: 10.1002/cyto.a.22652

© 2015 International Society for Advancement of Cytometry

• Abstract

Autophagy dysregulation has been implicated in numerous diseases and many therapeutic agents are known to modulate this pathway. Therefore, the ability to accurately monitor autophagy is critical to understanding its role in the pathogenesis and treatment of many diseases. Recently an imaging flow cytometry method measuring colocalization of microtubule associated protein 1B light chain 3 (LC3) and lysosomal signals via Bright Detail Similarity (BDS) was proposed which enabled evaluation of autophagic processing. However, since BDS only evaluates colocalization of LC3 and lysosomal signals, the number of autophagy organelles was not taken into account. We found that in cells classified as having Low BDS, there was a large degree of variability in accumulation of autophagosomes. Therefore, we developed a new approach wherein BDS was combined with number of LC3+ puncta, which enabled us to distinguish between cells having very few autophagy organelles versus cells with accumulation of autophagosomes or autolysosomes. Using this method, we were able to distinguish and quantify autophagosomes and autolysosomes in breast cancer cells cultured under basal conditions, with inhibition of autophagy using chloroquine, and with induction of autophagy using amino acid starvation. This technique yields additional insight into autophagy processing making it a useful supplement to current techniques. © 2015 International Society for Advancement of Cytometry

• Key terms

autophagy; autophagosome; autolysosome; imaging flow cytometry; LC3; spot count; LAMP1

AUTOPHAGY is an evolutionarily conserved cellular process for the degradation of long lived proteins, mis-folded proteins, and damaged cytoplasmic organelles (1). Autophagy dysregulation has been implicated in numerous diseases and many therapeutic agents are known to modulate this pathway (2). Therefore, the ability to accurately monitor autophagy is critical to understanding its role in the pathogenesis and treatment of many diseases.

Accurate evaluation of autophagy is challenging and typically requires multiple modalities. Prevailing methods to assess autophagy are extensively reviewed (3,4). Briefly, immunoblotting or fluorescence microscopy are the most commonly used approaches to monitor levels of cytosolic microtubule associated protein 1A/1B light chain 3 (LC3-I), its lipidated form autophagosome associated lipidated form of LC3 (LC3-II), which is incorporated into the autophagosome membrane, and sequestosome 1 (SQSTM1, p62), an endogenous substrate of autophagic degradation (4). Additionally, enumerating LC3 positive puncta in cells can be used to measure autophagic processes (4,5).

Recently, the development of new techniques using imaging flow cytometry (e.g., ImageStream[®]) has emerged. In general, they employ ectopic expression of

fluorescently tagged LC3 constructs or antibody staining of LC3 and measure fluorescence intensity or enumerate fluorescent spots, which may be indicative of autophagosomes or autolysosomes. One approach measuring colocalization of LC3 and lysosomal signals was proposed, which enabled more accurate evaluation of autophagic flux. It was reported that cells with high bright detail similarity (BDS; a colocalization index) between LC3 and lysosomal associated membrane protein 1 (LAMP1) had higher levels of autophagy and conversely that cells with low BDS scores had lower levels of autophagy (6). However, we found that this was not entirely accurate when evaluating inhibition of autophagy where there is an accumulation of autophagosomes due to inhibition of their degradation. These cells had low BDS scores and were not distinguishable from cells with very few autophagy organelles present using BDS alone. To have a more accurate measure of autophagy, we augmented this new approach by combining BDS with number of LC3+ puncta to distinguish between cells with accumulation of autophagosomes or autolysosome, and cells with few or no autophagy organelles present.

MATERIALS AND METHODS

Cells and Culture Conditions

NT5 cells, a Her2/neu-expressing mammary carcinoma cell line (7), were maintained in basal media at 37°C with 5% CO₂. The basal media was composed of RPMI (Mediatech, Manassas, VA) supplemented with 20% heat inactivated fetal bovine serum, 1% L-glutamine (Mediatech, Manassas, VA), 1% nonessential amino acids (Hyclone, Pittsburgh, PA), 1% sodium pyruvate (Mediatech, Manassas, VA), 0.2% insulin (Novolin R, 100 units/ml, Novo Nordisk, Princeton, NJ), 0.5% penicillin-streptomycin (Hyclone, Pittsburgh, PA), and 0.02% gentamycin (Mediatech, Manassas, VA).

Treatments

For time kinetics, cells were incubated in basal media with 120 μ M chloroquine (CQ; MP Biomedicals, Santa Ana, CA) for treatment durations of 0, 0.5, 1, 2, or 4.5 h. For dose kinetics, cells were incubated in basal media with CQ concentrations of 0, 30, 60, or 240 μ M for 4.5 h. For starvation kinetic studies, cells were incubated in starvation media Hanks' balanced salt solution (Mediatech, Manassas, VA) with 120 μ M CQ for durations of 0, 0.5, 1, 2, or 4.5 h. For experiments, evaluating autophagic flux under basal conditions and under starvation conditions, cells were incubated for 4.5 h in the respective media, in the presence of 120 μ M CQ or in the absence of CQ. Methods for estimating autophagic flux are further described below under imaging flow cytometry. At the end of the treatment periods, cells were collected after trypsinization, split in half and immediately processed for immunoblotting and imaging flow cytometry.

Staining and Antibodies

Cells were fixed in 1% paraformaldehyde and permeabilized in 0.005% saponin (Sigma-Aldrich, St. Louis, MO) in phosphate buffered saline (PBS; perm buffer). These cells were first stained using mouse anti-LC3 antibody (MBL, Woburn,

MA) at 1:100 dilution in perm buffer. This antibody is reactive against both LC3-I and LC3-II. Goat anti-mouse Alexa Fluor 488 was used as the secondary antibody (Invitrogen, Carlsbad, CA) at 1:200 dilution in PBS with 0.5% bovine serum albumin, then samples were stained with rat anti-mouse LAMP1 directly conjugated to phycoerythrin (BioLegend, San Diego, CA) at 1:200 dilution in perm buffer. All antibody incubations were done for 30 min on ice in the dark.

Imaging Flow Cytometry

The ImageStream^X (Amnis, Seattle, WA) one camera system with 488 and 658 nm lasers was used for imaging flow cytometry. The system was calibrated using bead standards (Amnis, Seattle, WA) prior to use and samples were acquired at optimized laser strength (100 mW for 488) with an area classifier (number of pixels in μm^2) set at 50. Images (LC3 in channel 2, LAMP1 in channel 3, and bright field in either channel 1 or 4) were acquired for each cell at 40 \times magnification and \sim 10,000 cells were analyzed for each experimental or isotype control sample, and 2,000 cells were acquired for each single positive compensation control sample. The integrated software INSPIRE (version 6.0.154, Amnis) was used for data collection and data were stored as raw image files, which were later compensated using a compensation matrix generated from the single positive controls. Analysis was performed on the compensated image files using algorithms in IDEAS (version 4.1.146, Amnis) image analysis software.

As with traditional flow cytometry, gating was determined for each experiment and cut-offs were defined by a negative biological control (cells cultured under basal conditions), similar to methods previously described by others (6,8). The bright field gradient root mean square (GRMS) feature was used to gate on cells that were in focus. Then bright field area versus aspect ratio features were plotted and used to gate on single cells (Supporting Information Fig. S1A). Cells with saturated pixels for LC3 or LAMP1 were excluded from the analysis by plotting the histogram for the Saturation Count feature (number of saturated pixels in each cell) and gating only on cells with 0 saturation count. All single and focused cells used in our analysis had zero saturated pixels (Supporting Information Fig. S1B). LC3 positive spots were identified by creating a spot mask for peak intensities that were greater than background. The peak to background ratio was determined for each experiment based on negative biological controls (untreated cells) and isotype staining controls. This spot mask was then converted into a spot count feature. The BDS R3 feature was used to measure colocalization based on over-lapping pixel intensities for LC3 and LAMP1 bright detail, using the default MC mask, a union of the pixels from all the channel masks. The LC3 spot counts, LAMP1 spot counts and BDS scores were plotted against a normalized frequency of cells to generate histograms. In addition, scatter plots of the number of LC3 positive puncta and BDS score were generated and three regions were gated around cell populations with high number of LC3 positive puncta and low BDS (autophagosomes), high number of LC3 positive puncta and high BDS (autolysosomes), or low number of LC3

positive puncta (few or no autophagy associated organelles). Example plots and gates are in Supporting Information Figure S1.

Rates of autophagosome processing (i.e., flux) were estimated by calculating the fold-change in autophagosomes in samples treated in the presence and the absence of CQ. The sample treated in the absence of CQ was taken as the denominator and the sample treated in the presence of CQ was taken as the numerator. Autophagic flux was estimated for cells cultured in basal media and in starvation media.

Immunoblotting

Cells were lysed in ice cold radio-immunoprecipitation assay (RIPA) buffer (Cell Signaling, Danvers, MA) supplemented with protease and phosphatase inhibitors (Sigma-Aldrich, St. Louis, MO) and 30 μg of total protein/sample was run on a 12% bis-tris gel (Novex, Life Technologies, Carlsbad, CA) under reducing conditions. Separated proteins were blotted onto a nitrocellulose membrane (Invitrogen, Carlsbad, CA) and blocked with 5% nonfat milk in tris-buffered saline with 0.1% Tween-20. Membranes were cut and separately probed with rabbit anti-mouse LC3-B (Cell Signaling, Danvers, MA) at 1:1,000 dilution or rabbit anti-mouse p62/sequestosome 1 (Cell Signaling, Danvers, MA) at 1:2,000 dilution in blocking buffer, overnight at 4°C with gentle agitation. The anti-LC3 antibody used is reactive against both LC3-I and LC3-II, with stronger reactivity against the latter. For both primary antibodies, the secondary antibody was goat anti-rabbit-HRP (Pierce-Thermo Scientific, Waltham, MA) at 1:10,000 incubated for 1 hour at room temperature. As a loading control, β -actin was probed with HRP-conjugated antibody (Sigma-Aldrich, St. Louis, MO) at 1:500,000 dilution. A chemiluminescent detection method was used and images acquired on BioSpectrum[®] 600 (UVP, Upland, CA) were used for densitometry analysis with ImageJ software (version 1.46r, NIH).

Statistical Analysis

Data with multiple groups were analyzed using one-way ANOVA, if $P < 0.05$ then post hoc testing was performed with Bonferroni correction for multiple comparisons (GraphPad Prism Software version 6.01). Comparisons were made to the untreated control groups, and differences were considered statistically significant if adjusted $P < 0.05$. Where there are only two groups, data were analyzed using unpaired two-tailed t test. Where applicable, data are expressed as mean \pm standard error of the mean (SEM) from at least three replicates.

RESULTS

LC3 Spot Counting and BDS as Measures of Autophagy Dynamics

We used a previously published imaging flow cytometry method to compare BDS score in NT5 breast cancer cells cultured under basal conditions and cells cultured in the presence of CQ, an autophagy inhibitor (Fig. 1A). As expected, we found that cells cultured under basal conditions had very low

BDS scores, similar to previously published findings. However, most cells cultured in the presence of CQ also had very low BDS scores, although there was a slight increase in BDS score, which could indicate alterations in autophagy. Most of the CQ treated cells classified as having low BDS scores had accumulation of only autophagosomes (Fig. 1B; LC3 single positive puncta) or lysosomes (Fig. 1C; LAMP1 single positive puncta) and very few autolysosomes (i.e., puncta that are double positive for LC3 and LAMP1). However, some cells with low BDS actually had very high numbers of single and double positive spots (Fig. 1D) indicative of high numbers of autophagosomes and autolysosomes. Conversely, while most cells with high BDS scores had high numbers of autolysosomes (Fig. 1E), some actually had very few LC3 positive spots (Fig. 1F). Importantly, using BDS alone may be insufficient since it is not able to distinguish between cells with and without accumulation of autophagosomes within the low BDS population.

To have a more accurate measure of autophagy, we evaluated LC3 and LAMP1 spot count (Fig. 2A) in addition to BDS. We found that CQ treatment increased number of LC3+ spots but had little impact on number of LAMP1+ spots. Therefore, we combined the two features, BDS and LC3 spot count and gated on three distinct regions (Fig. 2B). The two regions with populations of cells having high LC3 spots, were further classified into those with low versus high colocalization (BDS) between LC3 and LAMP1, representing autophagosomes (Fig. 2C, top, High Spot Low BDS) and autolysosomes (Fig. 2C, middle, High Spot High BDS), respectively. We interpreted high LC3 spots and low BDS to be indicative of autophagosome accumulation, whereas high LC3 spots and high BDS was indicative of autolysosome accumulation (Table 1). The third region consisted of cells with very few LC3 spots (Fig. 2C, bottom, Low Spot). Unlike using BDS alone, combining it with LC3 spot count revealed that under basal conditions, the majority of cells with low BDS had very few autophagosomes. Whereas treatment with CQ led to a significant increase in number of autophagosomes in the low BDS population.

To validate our assay as a method to monitor autophagy, we performed kinetic studies in NT5 cells cultured with or without CQ. Under basal conditions, numbers of autophagosomes and autolysosomes were low and few cells were found in the “high spots” region. As expected, increasing the dose of CQ from 30 to 240 μM led to a corresponding increase in autophagosomes (Fig. 3A, top) as measured using imaging flow cytometry, and accumulation of p62 (Fig. 3A, bottom) as measured by immunoblotting. Together, these data indicate that autophagy was inhibited. In our time studies, we observed that increasing the duration of CQ treatment from 30 min to 4.5 h led to a corresponding accumulation of autophagosomes (Fig. 3B, top) and p62 (Fig. 3B, bottom). The number of autolysosomes was not significantly altered by CQ treatment dose or duration (Supporting Information Fig. S2A and S2B). These results are consistent with CQ's reported mechanism of autophagy inhibition through inhibition of autophagosome and lysosome fusion, which would lead to

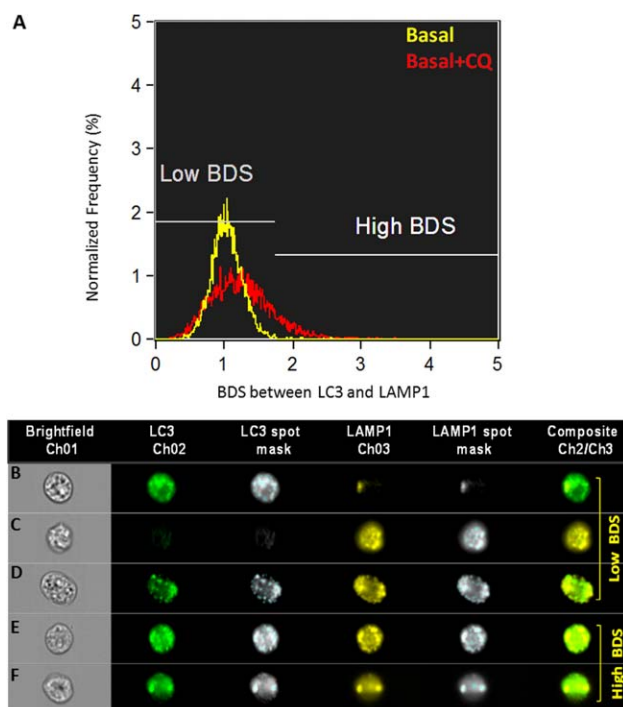


Figure 1. Evaluating autophagosomes and autolysosomes using imaging flow cytometry. NT5 tumor cells were cultured for 4.5 h under standard conditions in the absence (yellow population) and presence (red population) of 120 μ M CQ, then stained for LC3 (green fluorescence), and LAMP1 (yellow fluorescence). **A:** LC3 and LAMP1 colocalization (BDS) was plotted according to previously published methods. Representative images of cells from samples treated with CQ showing variability in number of LC3 and LAMP1 spots in cells with low BDS (**B–D**) and those with high BDS (**E,F**). Spot masks (blue spots) indicate LC3 or LAMP1 positive puncta that were recognized and counted by the image analysis algorithms. [Color figure can be viewed in the online issue, which is available at wileyonlinelibrary.com.]

significant accumulation of autophagosomes and likely not affect number of autolysosomes.

We next applied this technique to the evaluation of autophagy in NT5 cells under amino-acid starvation, which is reported to induce autophagy. Surprisingly, we observed a decrease in number of autophagosomes under starvation conditions rather than an increase (Figs. 4A and 4B, left), which may indicate that autophagy was not induced or conversely, that rates of autophagic degradation were increased thus few of these organelles have accumulated. We therefore estimated the autophagy processing rates (flux) by comparing the fold-change in autophagosome accumulation in the presence and absence of CQ, for starved cells and cells in basal media. These results show that the fold-increase was greater under starvation conditions compared to basal conditions (Fig. 4B, right), supporting that the rate of autophagy degradation was increased in starved cells.

Table 1. Interpretation of imaging flow cytometry data

LC3 ⁺ PUNCTA NUMBER	BDS SCORE (LC3 AND LAMP1 COLOCALIZATION)	INTERPRETATION
Low	Low	Few autophagosomes and autolysosomes present
High	Low	Accumulation of autophagosomes
High	High	Accumulation of autolysosomes

To verify our imaging flow cytometry findings, an aliquot of each sample was also processed to obtain lysate for immunoblot analysis of p62, LC3-I, and LC3-II protein levels (Fig. 4C). These results show that in basal media, CQ led to an accumulation of p62, LC3-I, and LC3-II as compared with untreated basal controls (Fig. 4D). This is consistent with our imaging flow cytometry findings showing that CQ inhibited autophagic processing. Under starvation conditions, immunoblot results revealed decreased levels of p62 and LC3-I compared to untreated basal controls (Fig. 4D) which supports that autophagy was induced by starvation. Additionally, LC3-II levels were not detectable, which is consistent with our imaging flow cytometry results showing very little accumulation of autophagosomes or autolysosomes. Since LC3-II is also degraded with the autophagosome contents, prolonged starvation conditions similar to the one above can paradoxically lead to decreased levels of LC3-II. In the presence of CQ, levels of p62 and LC3-I were lower for starved cells as compared to cells in basal media (Figs. 4C and 4D) indicating that CQ only partially blocked autophagic degradation when there was concurrent autophagy induction by starvation.

To further verify that starvation induced autophagy even in the presence of CQ, cells were starved in the presence of CQ and analyzed at multiple time points. These results show that initially there was a significant increase in number of autophagosomes evident after 30 min, which then steadily decreased (Fig. 5, top). In addition, immunoblot analysis

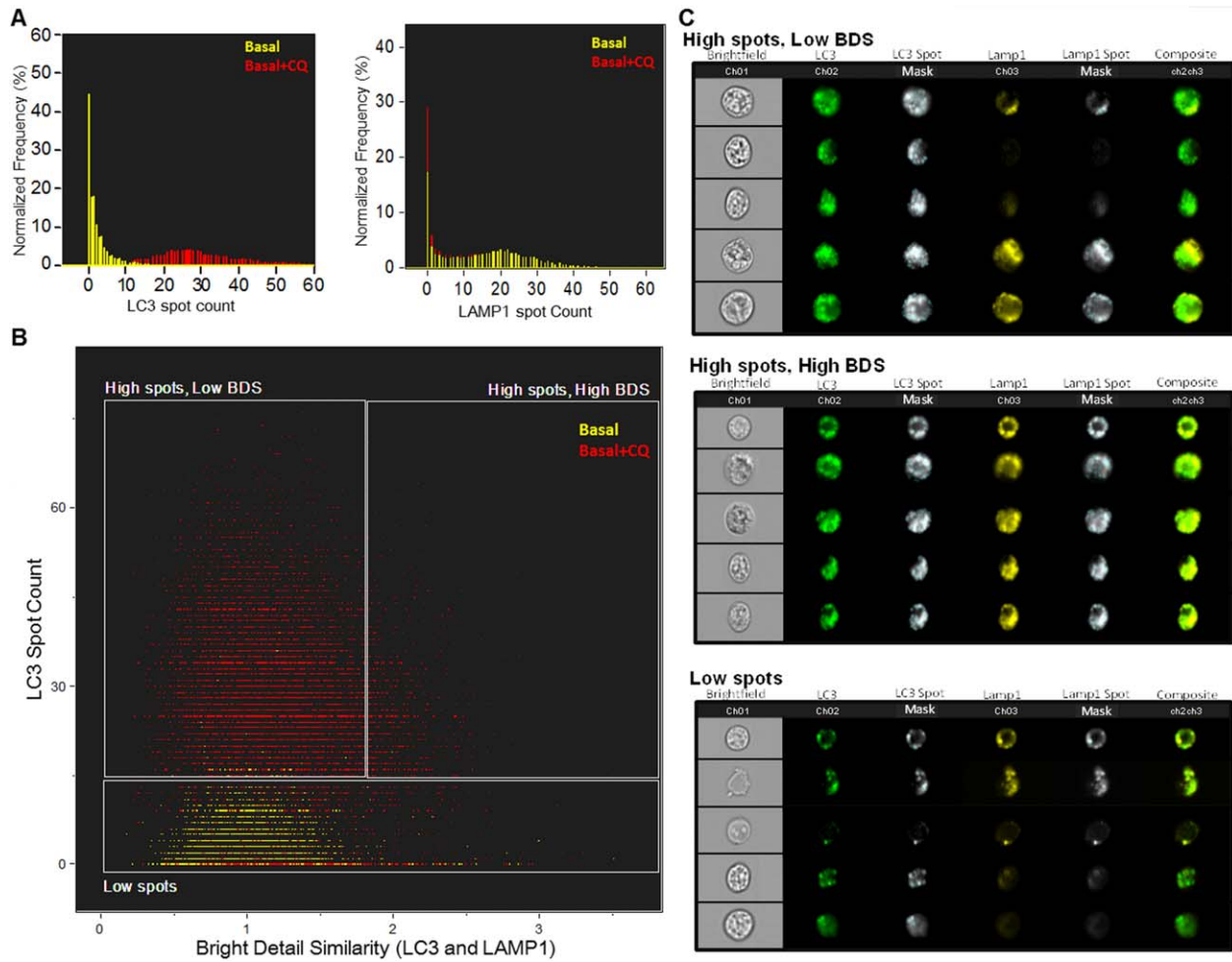


Figure 2. Gating and analysis strategies for evaluating autophagosomes and autolysosomes using imaging flow cytometry. NT5 tumor cells were cultured for 4.5 h under standard conditions in the absence (yellow population) and presence (red population) of 120 μ M CQ then stained for LC3 (green fluorescence) and LAMP1 (yellow fluorescence). **A** (left): The number of LC3+ puncta increased with CQ treatment compared with basal control. **A** (right): The number of LAMP1 puncta did not shift significantly with CQ treatment. **B**: Three distinct gated regions based on LC3 spot count and BDS shows the distribution of cell population treated with and without CQ. **C**: Representative images of cells from the three gated populations. [Color figure can be viewed in the online issue, which is available at wileyonlinelibrary.com.]

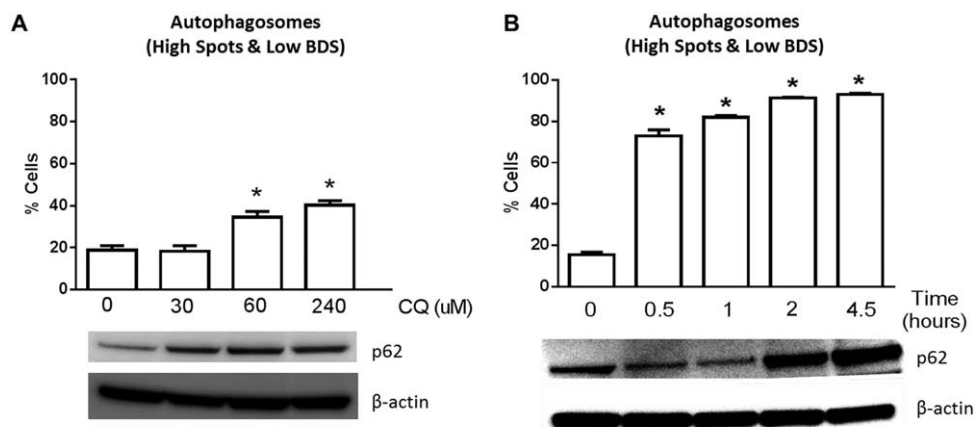


Figure 3. **A**: Concentration and **B**) time dependent accumulation of autophagosomes and p62 in NT5 cells treated with CQ. Cells were incubated with increasing concentrations of CQ (30 to 240 μ M) for 4.5 h (A) or cells were incubated with 120 μ M CQ for increasing durations (0.5–4.5 h). Data are mean \pm SEM of at least three replicates. (*indicates $P < 0.05$ using ANOVA-Bonferroni correction for multiple comparisons; all comparisons are to the untreated control group).

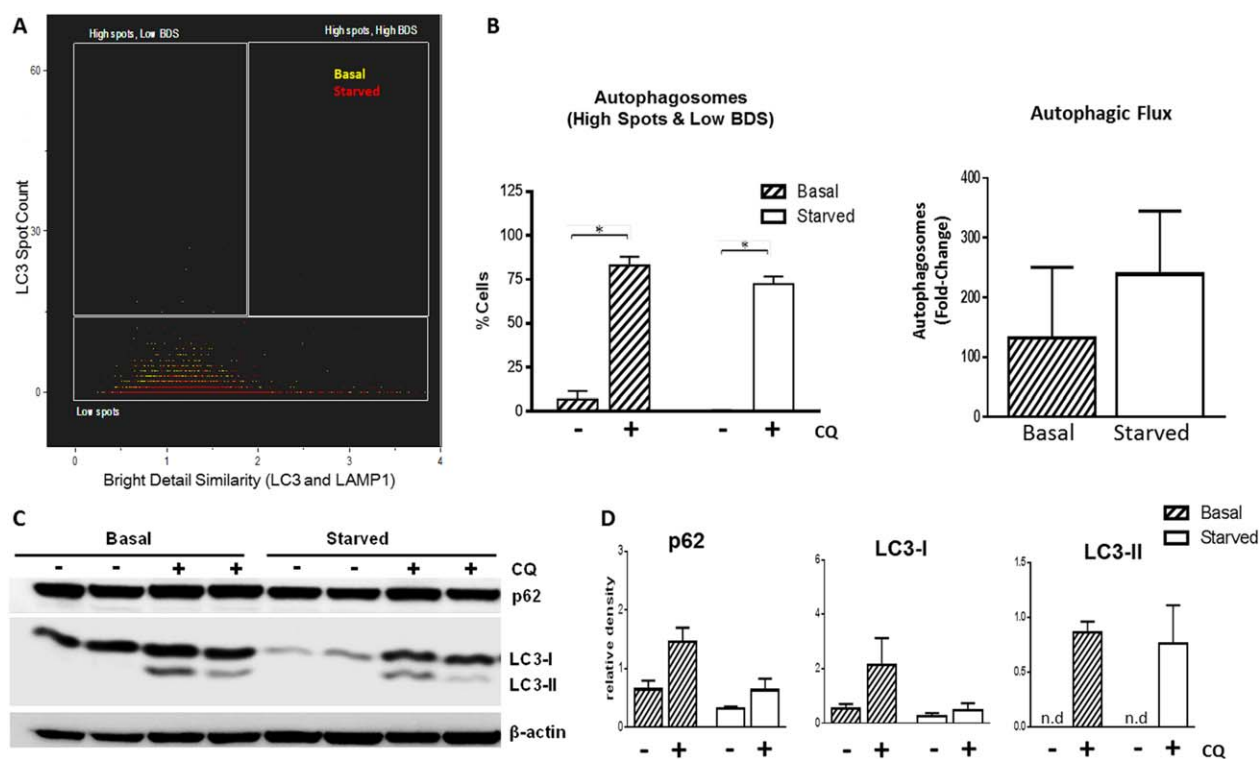


Figure 4. **A:** Representative plot of LC3+ spots versus LC3 and LAMP1 colocalization (BDS) in NT5 cells under basal culture conditions (yellow population) and under amino acid starvation (red population) for 4.5 h. Starvation did not increase number of autophagy organelles. **B:** In the presence of 120 μ M CQ, there was an increase in autophagosomes for cells cultured in both basal and starvation media. The fold-increase in autophagosomes was greater under starvation conditions than in basal media, suggesting that rates of autophagy processing were increased. **C:** Representative image of immunoblot analyses of p62, LC3-I, and LC3-II levels in the same samples. **D:** Relative density histograms from immunoblot analyses show that starvation decreased levels of p62 and LC3-I, supporting that autophagy was induced. CQ cotreatment led to an increase in p62, LC3-I, and LC3-II consistent with imaging flow cytometry results indicating that autophagic turnover was inhibited by CQ and that there was accumulation of autophagosomes and autolysosomes. Data are mean \pm SEM of at least three replicates (*indicates $P < 0.05$ using unpaired two-tailed t test; n.d., not detectable). [Color figure can be viewed in the online issue, which is available at wileyonlinelibrary.com.]

showed a steady decline in p62 levels (Fig. 5, bottom) which further supports that autophagy was induced and only partially blocked by CQ. Together, these data suggest amino acid starvation led to increased autophagic turnover rates, rather than that autophagy was not induced.

DISCUSSION

Using a recently published imaging flow cytometry assay (6) to evaluate the effects of CQ on autophagy in NT5 cells, we observed only a small increase in LC3 and LAMP1 colocalization (BDS) which was difficult to interpret. It was previously proposed that an increase in BDS was indicative of increased autophagic flux (6) but this interpretation was inconsistent with CQ’s mechanism of autophagy inhibition. Therefore, we proceeded to visually inspect the cells in the low and high BDS regions and found that using BDS alone can lead to false positive or false negative findings. Since BDS only evaluates LC3 and LAMP1 colocalization, the number of autophagy organelles was not taken into account. We found that in cells classified as having low BDS, there was a large degree of variability in number of autophagosomes. Therefore, we developed a new approach wherein BDS was com-

bined with number of LC3+ puncta, which enabled us to distinguish between cells having very few autophagy organelles versus cells with accumulation of autophagosomes within the Low BDS population. We validated our imaging flow cytometry approach by performing kinetic studies with CQ, which showed dose and time dependent accumulation of autophagosomes, indicative of autophagy inhibition. These findings were further verified by immunoblot analysis showing dose and time dependent accumulation of p62, an autophagy substrate.

Interestingly, amino acid starvation did not lead to an accumulation of autophagosomes in our imaging flow cytometry assay nor an increase in LC3-II in our immunoblot analyses. However, there was a decrease in p62 and LC3-I, which would suggest that autophagy was induced and the lack of autophagosomes may be due to an increase in rates of autophagic turnover. When cells were starved in the presence of CQ, the fold-increase in autophagosomes and autolysosomes was greater than the fold-increase observed for cells cultured in basal media with and without CQ, which further supports our conclusion that amino acid starvation increased autophagic flux. Other possible explanations for the lack of accumulation of autophagosomes and LC3-II include factors such as

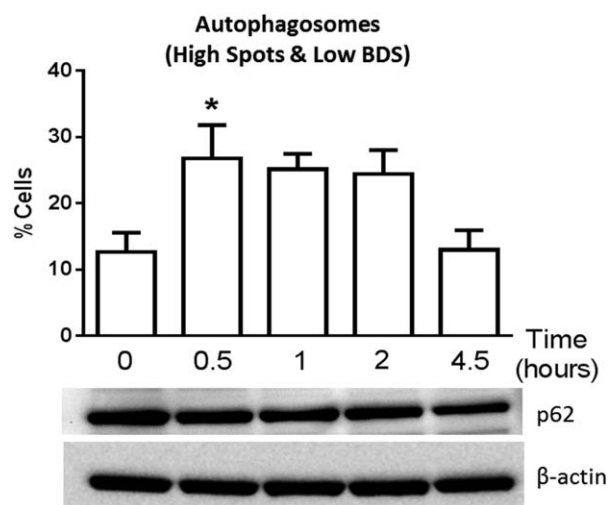


Figure 5. NT5 cells were starved in the presence of 120 μ M CQ and analyzed at multiple time points. Autophagosomes accumulated early on but then steadily declined suggesting that autophagy was induced by amino-acid starvation. Immunoblot analysis shows a steady decrease in p62, which further supports that autophagy was induced and only partially blocked by CQ. Data are mean \pm SEM of at least three replicates. (*indicates $P < 0.05$ using ANOVA-Bonferroni correction for multiple comparisons; all comparisons are to the untreated control group).

degradation of LC3-II itself with prolonged induction of autophagy, differential affinities of antibodies to LC3-I compared with LC3-II, and differences in expression levels of these two isoforms among cell lines and tissues.

Our imaging flow cytometry results do not mirror exactly our immunoblot data although they follow similar trends. The differences in results between the imaging flow cytometry and immunoblot methods are likely due to the differences in assay sensitivity, and data input and output. For example, our imaging assay evaluates the presence of autophagy organelles in individual cells and the resulting read-out is a measure of autophagic turnover of these vesicles in a specific population of cells. In contrast, immunoblotting evaluates the overall turnover of substrates for autophagic degradation in a bulk sample.

The results from LC3 immunoblot analysis are challenging to interpret (9). The anti-LC3 antibody used here is typical of antibodies used for immunoblot analysis in that they tend to be cross reactive with both LC3-I and LC3-II. However, due to the different extraction efficiencies between LC3-I and LC3-II, and their different antibody reactivity, it would be difficult to evaluate cellular autophagy using LC3 immunoblot since their proportionality cannot be assumed (9). In addition, LC3-II itself is a substrate for autophagic degradation thus while induction of autophagy is expected to increase LC3-II, prolonged induction may actually lead to a decrease in LC3-II levels. Thus there is a need to develop alternative methods to monitor autophagy such as our imaging flow cytometry approach which overcomes some of these limitations. Although the antibody used in our imaging assay is also cross reactive with LC3-I and LC3-II, the bright detail and

spot count algorithms enable us to distinguish between the diffuse fluorescence signal of cytosolic LC3 (LC3-I) and the punctate and brighter signal of autophagic LC3 (LC3-II). Moreover, unlike immunoblotting, our imaging assay enables the direct visualization and quantitation of autophagy organelles at the level of individual cells.

There is increasing evidence that p62 may be degraded through the ubiquitin-proteasome pathway (10–12) and that autophagy modulators, such as CQ, may also affect this and other pathways (12–15). Hence, even adding p62 to LC3 immunoblot alone would not be sufficient (3). However, combining p62 immunoblot with imaging assays such as ours to query the presence of autophagosomes and autolysosomes would yield more insight into autophagic processes. In our studies, combining imaging flow cytometry and immunoblot enabled us to more accurately determine the impact of CQ treatment and amino acid starvation on autophagy as compared with either method alone.

Another advantage of our assay is that it can be used with both fluorescently tagged LC3 or with antibody stained samples. Accordingly, this makes it an ideal assay for clinical studies since it does not require any transfection, sample processing is relatively straightforward, and many steps are automated. A limitation of our method and others that use flow cytometry is that it requires cells in suspension. While in vitro investigations utilizing adherent cells can be readily processed to generate cells in suspension, this remains a challenge when evaluating autophagy in primary tissues.

In conclusion, we have expanded on a new assay for autophagy using imaging flow cytometry, enabling researchers to quantify and distinguish between autophagosomes and autolysosomes. This assay is rapid, statistically robust, and simpler than standard immunoblot and microscopy methods which can be technically demanding and labor intensive. In theory, it can be used to probe autophagosome and autolysosome turnover in distinct cell populations within a heterogeneous sample, when combined with cell-type specific markers (6). Moreover, this method can be used to gain additional insight into the execution of autophagy at two distinct steps within a population of cells: autophagosome formation and autolysosome formation. This information can be especially valuable while identifying alterations at different levels of the autophagy process that is affected by either regulatory effectors or therapeutic agents. Therefore, we believe that this imaging flow cytometry assay will be a useful supplement to other techniques for monitoring cellular autophagic processes.

LITERATURE CITED

- Levine B, Klionsky DJ. Development by self-digestion: Molecular mechanisms and biological functions of autophagy. *Dev Cell* 2004;6:463–477.
- Shintani T, Klionsky DJ. Autophagy in health and disease: A double-edged sword. *Science* 2004;306:990–995.
- Klionsky DJ, et al. Guidelines for the use and interpretation of assays for monitoring autophagy. *Autophagy* 2012;8:445–544.
- Mizushima N, Yoshimori T, Levine B. Methods in mammalian autophagy research. *Cell* 2010;140:313–326.
- Rubinsztein DC, Cuervo AM, Ravikumar B, Sarkar S, Korolchuk V, Kaushik S, Klionsky DJ. In search of an “autophagometer”. *Autophagy* 2009;5:585–589.
- Phadwal K, Alegre-Abarrategui J, Watson AS, Pike L, Anbalagan S, Hammond EM, Wade-Martins R, McMichael A, Klenerman P, Simon AK. A novel method for

- autophagy detection in primary cells: Impaired levels of macroautophagy in immunosenescent T cells. *Autophagy* 2012;8:677–689.
7. Reilly RT, Gottlieb MB, Ercolini AM, Machiels JP, Kane CE, Okoye FI, Muller WJ, Dixon KH, Jaffee EM. HER-2/neu is a tumor rejection target in tolerized HER-2/neu transgenic mice. *Cancer Res* 2000;60:3569–3576.
 8. de la Calle C, Joubert PE, Law HK, Hasan M, Albert ML. Simultaneous assessment of autophagy and apoptosis using multispectral imaging cytometry. *Autophagy* 2011;7:1045–1051.
 9. Mizushima N, Yoshimori T. How to interpret LC3 immunoblotting. *Autophagy* 2007;3:542–545.
 10. He C, Klionsky DJ. Regulation mechanisms and signaling pathways of autophagy. *Annu Rev Genet* 2009;43:67–93.
 11. Nakaso K, Yoshimoto Y, Nakano T, Takeshima T, Fukuhara Y, Yasui K, Araga S, Yanagawa T, Ishii T, Nakashima K. Transcriptional activation of p62/A170/ZIP during the formation of the aggregates: Possible mechanisms and the role in Lewy body formation in Parkinson's disease. *Brain Res* 2004;1012:42–51.
 12. Myeku N, Figueiredo-Pereira ME. Dynamics of the degradation of ubiquitinated proteins by proteasomes and autophagy: Association with sequestosome 1/p62. *J Biol Chem* 2011;286:22426–22440.
 13. Solomon VR, Lee H. Chloroquine and its analogs: A new promise of an old drug for effective and safe cancer therapies. *Eur J Pharmacol* 2009;625:220–233.
 14. Wu YT, Tan HL, Shui G, Bauvy C, Huang Q, Wenk MR, Ong CN, Codogno P, Shen HM. Dual role of 3-methyladenine in modulation of autophagy via different temporal patterns of inhibition on class I and III phosphoinositide 3-kinase. *J Biol Chem* 2010;285:10850–10861.
 15. Yang YP, Hu LF, Zheng HF, Mao CJ, Hu WD, Xiong KP, Wang F, Liu CF. Application and interpretation of current autophagy inhibitors and activators. *Acta Pharmacol Sin* 2013;34:625–635.